# Imaging Gastric Cancer with PET and the Radiotracers $^{18}$F-FLT and $^{18}$F-FDG: A Comparative Analysis

Ken Herrmann*[1], Katja Ott*[2], Andreas K. Buck[1], Florian Lordick[3], Dirk Wilhelm[2], Michael Souvatzoglou[1], Karen Becker[4], Tibor Schuster[5], Hans-Jürgen Wester[1], Jörg R. Siewert[2], Markus Schwaiger[1], and Bernd J. Krause[1]

*[1]Department of Nuclear Medicine, Technische Universität München, Munich, Germany; [2]Department of Surgery, Technische Universität München, Munich, Germany; [3]Department of Internal Medicine III, Technische Universität München, Munich, Germany; [4]Department of Pathology, Technische Universität München, Munich, Germany; and [5]Department of Medical Statistics, Technische Universität München, Munich, Germany*

In this pilot study, we evaluated 3′-deoxy-3′-$^{18}$F-fluorothymidine (FLT) PET for the detection of gastric cancer and compared the diagnostic accuracy with that of $^{18}$F-FDG PET. **Methods:** Forty-five patients (31 male and 14 female) with histologically proven locally advanced gastric cancer underwent attenuation-corrected whole-body $^{18}$F-FLT PET and $^{18}$F-FDG PET/CT (low-dose CT). $^{18}$F-FLT emission images were acquired on a full-ring PET scanner 45 min after the injection of 270–340 MBq of $^{18}$F-FLT. $^{18}$F-FDG PET/CT was performed 60 min after the injection of 300–370 MBq of $^{18}$F-FDG. Mean standardized uptake values for $^{18}$F-FLT and $^{18}$F-FDG were calculated using circular ROIs (diameter, 1.5 cm) in the primary tumor manifestation site, in a reference segment of the liver, and in the bone marrow and were compared on a lesion-by-lesion basis. **Results:** According to the Lauren classification, 15 tumors (33%) were of the intestinal subtype and 30 (67%) of the nonintestinal subtype. $^{18}$F-FLT PET images showed high contrast for the primary tumor and proliferating bone marrow. In all patients (45/45), focal $^{18}$F-FLT uptake could be detected in the primary tumor. In contrast, 14 primary tumors were negative for $^{18}$F-FDG uptake, with lesional $^{18}$F-FDG uptake lower than or similar to background activity. The mean standardized uptake value for $^{18}$F-FLT in malignant primaries was 6.0 ± 2.5 (range, 2.4–12.7). In the subgroup of $^{18}$F-FDG–positive patients, the mean value for $^{18}$F-FDG was 8.4 ± 4.1 (range, 3.8/19.0), versus 6.8 ± 2.6 for $^{18}$F-FLT (Wilcoxon test: $P = 0.03$). Comparison of mean $^{18}$F-FLT and $^{18}$F-FDG uptake in tumors with signet ring cells revealed no statistically significant difference between the tracers (6.2 ± 2.1 for $^{18}$F-FLT vs. 6.4 ± 2.8 for $^{18}$F-FDG; Wilcoxon test: $P = 0.94$). **Conclusion:** The results of this study indicate that imaging gastric cancer with the proliferation marker $^{18}$F-FLT is feasible. $^{18}$F-FLT PET was more sensitive than $^{18}$F-FDG PET, especially in tumors frequently presenting without or with low $^{18}$F-FDG uptake, and may improve early evaluation of response to neoadjuvant treatment.

Received Jul. 9, 2007; revision accepted Sep. 6, 2007.
For correspondence or reprints contact: Ken Herrmann, MD, Department of Nuclear Medicine, Technische Universität München, Ismaninger Str. 22, D-81675 Munich, Germany.
E-mail: ken.herrmann@web.de
*Contributed equally to this work.


**Key Words:** FLT; gastric cancer; proliferation; PET
**J Nucl Med 2007; 48:1945–1950**
DOI: 10.2967/jnumed.107.044867

Imaging of gastric cancer with $^{18}$F-FDG PET is limited because of the relatively high number of primary tumors that are not avid for $^{18}$F-FDG (4%–53%), making primary staging and early evaluation of response to treatment impossible (*1–5*). Published sensitivities for $^{18}$F-FDG PET range from 47% to 96% (mean sensitivity, 77%; mean specificity, 99%) for the detection of gastric cancer and from 23% to 73% (mean sensitivity, 45%; mean specificity, 92%) for the detection of lymph node involvement (*1–5*). $^{18}$F-FDG uptake has been shown to be lower in cancers of the nonintestinal type, with signet ring cells, high mucinous content, and lower cellularity (*3,6,7*).

To increase sensitivity and specificity for gastric cancer, other tracers that complement the information provided by $^{18}$F-FDG are required. Increased proliferative activity has been shown to be potentially more specific for malignant tumors than are alterations of glucose metabolism (*8*). Therefore, measurement of tumor growth and DNA synthesis in vivo might be superior for imaging malignancies of the gastrointestinal tract. Recently, the pyrimidine analog 3′-deoxy-3′-$^{18}$F-fluorothymidine (FLT) has been reported to be a stable PET tracer that accumulates in proliferating tissues and malignant tumors (*9*). $^{18}$F-FLT is a substrate for thymidine kinase 1, which is a key enzyme in the salvage pathway for the producing of thymidine monophosphate and has been assessed for its potential role in imaging thymidylate synthase inhibition (*10–12*). Several human studies recently demonstrated the feasibility of $^{18}$F-FLT PET for imaging gastrointestinal cancers (*13–15*).

In this pilot study, we investigated the feasibility of $^{18}$F-FLT PET, in comparison to $^{18}$F-FDG PET, for imaging locally advanced gastric cancer. Furthermore, we examined

the correlation of $^{18}$F-FLT uptake with the histologic subtype and location of the tumor.

## MATERIALS AND METHODS

### Patient Population

Forty-five consecutive patients with an initial diagnosis of locally advanced gastric cancer and meeting the eligibility requirements (presence of biopsy-proven gastric cancer with or without clinical evidence of locoregional lymph node metastases and with a tumor stage of T3–4, Nx, M0, according to the TNM classification system) were included in this prospective study (31 men and 14 women; mean age, 61 ± 11 y; range, 36–78 y). Staging procedures included endoscopy, endoscopic ultrasound, and CT of the chest, abdomen, and pelvis in all patients and additional laparoscopy in some patients. Tumors were localized with endoscopy and—if available and detectable—CT. Patients with an Eastern Cooperative Oncology Group score of less than 1, uncontrolled bleeding from the tumor, gastric outlet syndrome, or an age of less than 18 y were excluded. Details of the study were explained by a physician, and written informed consent was obtained from all patients. The study protocol was approved by the local ethics committee of the Technische Universität München.

### Histologic Classification

For histopathologic evaluation of the biopsy samples, the Lauren classification, tumor grading (microscopic growth type), and World Health Organization classification were applied. Tumor location was defined according to the findings on endoscopy and CT. In this study, a modified Lauren classification was used. This classification differentiates only between intestinal (gland formation) and nonintestinal tumors. This modification facilitates the classification based on biopsy and thereby decreases interobserver variability (*7,16*).

### $^{18}$F-FLT PET

$^{18}$F-FLT was synthesized as previously described (*17*). Imaging was performed on a whole-body high-resolution PET scanner (ECAT HR+; Siemens/CTI). This scanner simultaneously acquires 47 contiguous slices with a slice thickness of 3.4 mm. The in-plane image resolution of transaxial images was approximately 8 mm in full width at half maximum, with an axial resolution of approximately 5 mm in full width at half maximum.

A dynamic 45-min acquisition began simultaneously with the injection of approximately 300 MBq of $^{18}$F-FLT (range, 270–340 MBq). Twelve 10-s frames, three 1-min frames, and eight 5-min frames were acquired. After the dynamic phase, static emission images were acquired covering the abdominal and pelvic area (2-dimensional mode, 4–5 bed positions, 8 min for each). Emission data were corrected for random coincidences, dead time, and attenuation and were reconstructed by filtered backprojection (Hanning filter with a cutoff frequency of 0.4 cycles per bin). The matrix size was 128 × 128 pixels, with a pixel size of 4.0 × 4.0 mm. The image pixel counts were calibrated to activity concentrations (Bq/mL) and decay-corrected using the time of tracer injection as the reference.

### $^{18}$F-FDG PET/CT

Patients underwent $^{18}$F-FDG PET/CT on a Biograph Sensation 16 scanner (Siemens Medical Solutions). The CT protocol included acquisition of a low-dose CT scan (26 mAs, 120 kV, 0.5 s per rotation, and 5-mm slice thickness) from the base of the skull to the mid thigh for attenuation correction, with use of diluted oral contrast material (sodium meglumine ioxithalamate, 300 mg), followed by the PET scan. All PET scans were acquired in 3-dimensional mode with an acquisition time of 3 min per bed position. Forty-seven contiguous slices were acquired per bed position, and the matrix size was 128 × 128, with a slice thickness of 3.4 mm. Images were reconstructed using attenuation-weighted ordered-subsets expectation maximization algorithm (4 iterations and 8 subsets) followed by a postreconstruction smoothing gaussian filter (5 mm in full width at half maximum). Patients fasted at least 6 h before the PET scan, and blood glucose levels were measured before administration of $^{18}$F-FDG. All measured values were less than 150 mg/dL. Static emission imaging was performed 60 min after intravenous injection of 300–370 MBq of $^{18}$F-FDG. Emission data were corrected for randoms, dead time, scatter, and attenuation, and the same reconstruction algorithm was applied as for the conventional PET data.

### PET Data Analysis

All $^{18}$F-FLT PET scans were evaluated by 2 experienced nuclear medicine physicians who were unaware of the clinical data and the results of other imaging studies. Circular regions of interest (ROIs) with a diameter of 1.5 cm were placed in the area with the highest tumor activity as described earlier (*18*). Mean standardized uptake values (SUVs) were calculated from each ROI using the following formula: SUV = measured activity concentration (Bq/g) × body weight (g)/injected activity (Bq). ROIs were also placed in reference segments of the following organs: liver, bone marrow, and muscle. For definition of ROIs and data analysis, computer programs developed in the Interactive Data Language (IDL; Research Systems, Inc.) using the Clinical Application Programming Package (CAPP; Siemens/CTI, Inc.) (*19*).

$^{18}$F-FDG PET/CT scans were semiquantitatively evaluated by circular ROIs (diameter, 1.5 cm) with the eSOFT software (Siemens Medical Solutions) and normalized for injected dose and the patient's body weight.

### Statistical Analysis

Statistical analyses were performed using SPSS software (version 14.0; SPSS, Inc.). Quantitative values were expressed as mean ± SD, median, and range. Related metric measurements were compared using the Wilcoxon signed rank test and the Mann–Whitney *U* test in the case of 2 independent samples. The Fisher exact test was used for comparison of frequencies, and Spearman correlation coefficients were calculated to quantify bivariate correlations of measurement data. All analyses were 2-sided, and a *P* value of less than 0.05 was considered statistically significant.

## RESULTS

### Patients

The primary tumor was located in the proximal third of the stomach in 28 patients (62%), in the middle third in 9 patients (20%), and in the distal third in 8 patients (18%). According to the Lauren classification, 15 tumors (33%) were of the intestinal subtype and 30 (67%) of the nonintestinal subtype. Most tumors (78%) were poorly differentiated (grade 3 or 4 of 4). The endoscopic tumor category

was cT3 in all included patients. Two tumors were cN0, and 43 were cN+. Histologic sections showed signet ring cells in 27 patients (60%) and mucinous content in 18 patients (40%).

### Visual Interpretation of Gastric Cancer with $^{18}$F-FLT PET and $^{18}$F-FDG PET/CT

In the 45 patients undergoing an initial $^{18}$F-FLT PET scan, all tumors showed focal uptake of $^{18}$F-FLT, resulting in a sensitivity of 100%. Background activity was low for $^{18}$F-FLT, resulting in a high tumor-to-background contrast. In the $^{18}$F-FDG PET/CT scan, only 31 of 45 tumors could be detected visually, resulting in a sensitivity of 69% and a significantly lower detection rate than for $^{18}$F-FLT ($P < 0.01$) (Table 1). Uptake in the $^{18}$F-FDG–avid tumors was much higher than the physiologically variable uptake in the gastric wall.

### Semiquantitative Evaluation of $^{18}$F-FLT Uptake and Biodistribution

In all 45 patients, focal $^{18}$F-FLT uptake could be detected in the region of histologically proven gastric cancer. The mean $^{18}$F-FLT uptake ($^{18}$F-FLT SUV) of the tumor sites was 6.0 ± 2.5 (median, 5.3; range, 2.4–12.7). Besides tracer accumulation in the tumor, high physiologic $^{18}$F-FLT uptake in proliferating bone marrow was observed (mean SUV, 7.4; median, 7.2; range, 3.7–10.6). The mean $^{18}$F-FLT SUV in a reference segment was 5.3 for liver (median, 4.9; range, 2.9–13.2) and 0.9 for muscle (median, 0.9; range, 0.4–1.3). Figure 1 illustrates the biodistribution of $^{18}$F-FLT in patients with gastric cancer.

Focal $^{18}$F-FLT uptake in the tumor sites showed no significant dependence on location (proximal third, 6.1, vs. distal thirds, 5.9; $P = 0.87$), Lauren classification (intestinal subtype, 7.1, vs. nonintestinal subtype, 5.5; $P = 0.11$), or presence of mucinous cells (mucin-positive, 6.1, vs. mucin-negative, 6.0; $P = 0.65$). In contrast, the subgroup of tumors with signet ring cells had a significantly lower $^{18}$F-FLT uptake than did tumors without signet ring cells (5.4 vs. 7.0; $P = 0.05$).

### Imaging with $^{18}$F-FDG PET/CT

In 14 of the 45 patients, the primary tumor was not detectable with $^{18}$F-FDG PET/CT (Table 1). Tumors with insufficient image contrast had signet ring cells more often than did $^{18}$F-FDG–positive tumors (11/14 [79%] vs. 16/31 [52%]), but this difference was not statistically significant ($P = 0.09$). Additionally, there was a tendency toward a higher proportion of $^{18}$F-FDG PET–negative tumors in the middle and distal thirds than in the proximal third of the stomach (8/14 [57%]), compared with $^{18}$F-FDG–positive tumors, but statistical significance was not reached (9/31 [29%]; $P = 0.07$).

Mean $^{18}$F-FDG uptake for the $^{18}$F-FDG–positive tumors was 8.4 ± 4.1 (median, 7.1; range, 3.8–19.0). The subgroup of $^{18}$F-FDG–positive tumors with signet ring cells had a significantly lower $^{18}$F-FDG uptake than did tumors without signet ring cells (6.4 vs. 10.7; $P < 0.01$). Additionally, tumoral $^{18}$F-FDG uptake correlated significantly with the Lauren classification. Tumors of the intestinal subtype had a significantly higher $^{18}$F-FDG uptake than did nonintestinal tumors (10.5 vs. 7.2; $P < 0.01$). In contrast, a difference in uptake dependent on the location (8.3 vs. 8.9; $P = 0.62$) and on the presence of mucinous content (8.3 vs. 8.5; $P = 0.48$) was not statistically significant.

### Comparison of $^{18}$F-FLT and $^{18}$F-FDG Uptake

Analyzing all patients with an $^{18}$F-FDG uptake in gastric cancer higher than background activity ($n = 31$) showed a significant correlation between the mean SUVs of the 2 radiotracers studied ($^{18}$F-FLT, 6.8 ± 2.6, vs. $^{18}$F-FDG, 8.4 ± 4.1; $r = 0.46$; $P < 0.01$) (Figs. 2 and 3). Despite this correlation, initial $^{18}$F-FDG uptake was significantly higher than initial $^{18}$F-FLT uptake for both mean SUV ($P = 0.03$) and maximum SUV (7.8 ± 3.0 vs. 11.5 ± 5.6; $P < 0.01$). In contrast, in the subgroup of signet ring cell–positive tumors ($n = 27$), there was no significant difference between $^{18}$F-FLT and $^{18}$F-FDG uptake as indicated by mean SUV ($^{18}$F-FLT, 6.2 ± 2.1, vs. $^{18}$F-FDG, 6.4 ± 2.8; $P = 0.94$) or by maximum SUV ($^{18}$F-FLT, 7.2 ± 2.6, vs. $^{18}$F-FDG, 8.4 ± 3.4; $P = 0.07$). Uptake of the 2 tracers showed no significant correlation in this subgroup ($r = 0.38$; $P = 0.15$) (Fig. 2). In the subgroup of $^{18}$F-FDG–negative tumors, the mean SUV of focal $^{18}$F-FLT uptake was 4.2 ± 1.2 (Table 1).

## DISCUSSION

This clinical study demonstrated the potential of $^{18}$F-FLT PET for imaging gastric cancer. In contrast to the standard

**TABLE 1**
Sensitivity and Uptake of $^{18}$F-FLT and $^{18}$F-FDG in Gastric Cancer

| Index | $^{18}$F-FLT | $^{18}$F-FDG |
|---|---|---|
| Overall sensitivity | 100% (45/45) | 69% (31/45) ($P < 0.01$) |
| Sensitivity for SRC-positive | 100% (27/27) | 59% (16/27) ($P < 0.01$) |
| Sensitivity for non-SRC | 100% (18/18) | 83% (15/18) ($P = 0.23$) |
| Overall mean SUV | 6.0 ± 2.5 | NA |
| Mean SUV for $^{18}$F-FDG–positive | 6.8 ± 2.6 | 8.4 ± 4.1 ($P = 0.03$) |
| Mean SUV for $^{18}$F-FDG–negative | 4.2 ± 1.2 | NA |

SRC = signet ring cell carcinoma; NA = not applicable.

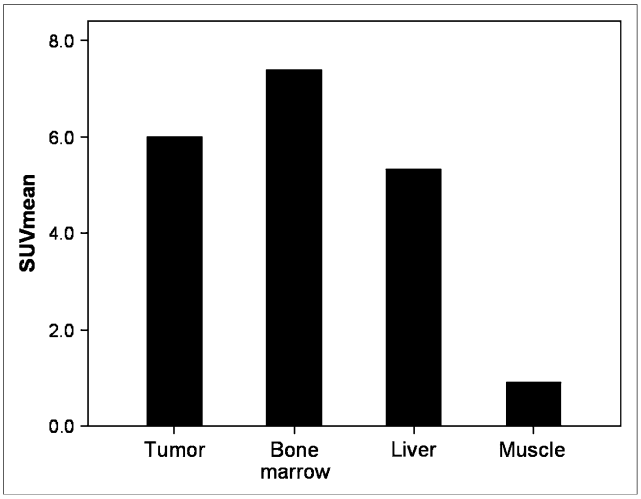


**FIGURE 1.** Biodistribution of $^{18}$F-FLT in all patients.

radiotracer $^{18}$F-FDG, $^{18}$F-FLT was able to detect all locally advanced gastric cancers with sufficient contrast for quantification. Therefore, $^{18}$F-FLT may represent a superior radiotracer for visualization of stomach cancer, especially of histologic subtypes that frequently have low or no $^{18}$F-FDG uptake, as well as for response evaluation. Uptake of $^{18}$F-FLT in the malignant primary correlated significantly with the corresponding $^{18}$F-FDG uptake ($r = 0.46$); however, mean and maximum $^{18}$F-FDG SUV were significantly higher than the corresponding $^{18}$F-FLT values. This observation is in line with studies reporting higher uptake of $^{18}$F-FDG than of $^{18}$F-FLT in other solid tumors such as esophageal or lung cancer (*14,20*).

Interestingly, even $^{18}$F-FDG–negative tumors with signet ring cells or mucinous content were detected by $^{18}$F-FLT PET. Compared with tumors responding to neoadjuvant chemotherapy (as indicated by a rapid decrease in tumoral $^{18}$F-FDG uptake), signet ring cell–positive tumors are characterized by a different biological behavior resulting in lower response rates and impaired prognosis (*21*). Increased consumption of glucose is characteristic of most cancers and is in part related to overexpression of glucose transporters (*22*). As rationale for $^{18}$F-FDG–negative gastric tumors, it has been postulated that the low or absent $^{18}$F-FDG uptake in the nonintestinal subtype results from the high number of signet ring cells, leading to a reduced $^{18}$F-FDG concentration in the tumor. Another reason could be the lack of expression of the glucose transporter Glut-1 on the cell membrane of most nonintestinal gastric cancer tumors (*23*).

There was also a trend toward lower detection rates of $^{18}$F-FDG PET in the middle and distal thirds than in the proximal third of the stomach ($P = 0.07$, nonsignificant). This observation could be explained by the low or absent $^{18}$F-FDG uptake in the nonintestinal subtype resulting from the high number of signet ring cells. Compared with intestinal gastric cancer, nonintestinal gastric cancer shows a higher chromosomal stability, which might lead to a lower proliferation rate. Nonintestinal gastric cancer is characterized by a lower fractional allelic loss and a lower loss of heterozygosity being inversely correlated with the methylation rate (*24*). Nonintestinal tumors with a high methylation rate and low fractional allelic loss and loss of heterozygosity tend to have a worse prognosis than do intestinal tumors (*24,25*). Chromosomally stable tumors might show lower proliferative activity. Therefore, antiproliferative agents might be less effective, potentially leading to lower response rates in nonintestinal tumors.

In contrast to $^{18}$F-FDG, $^{18}$F-FLT PET specifically reflects activity of thymidine kinase 1, the key enzyme of the salvage pathway for producing thymidine monophosphate. The level of thymidine kinase 1 protein has proven to be an important determinant of $^{18}$F-FLT uptake in tumors. However, the detailed uptake mechanism remains to be determined. A recent study showed that $^{18}$F-FLT PET can be used to measure thymidylate synthase inhibition in tumors early after drug administration, indicating a potential use of $^{18}$F-FLT for early measurement of antiproliferative drug effects (*26*). There was a trend toward lower tumoral $^{18}$F-FLT uptake in nonintestinal than intestinal tumors, according to the Lauren classification. However, the presence of signet ring cells was the only histopathologic factor

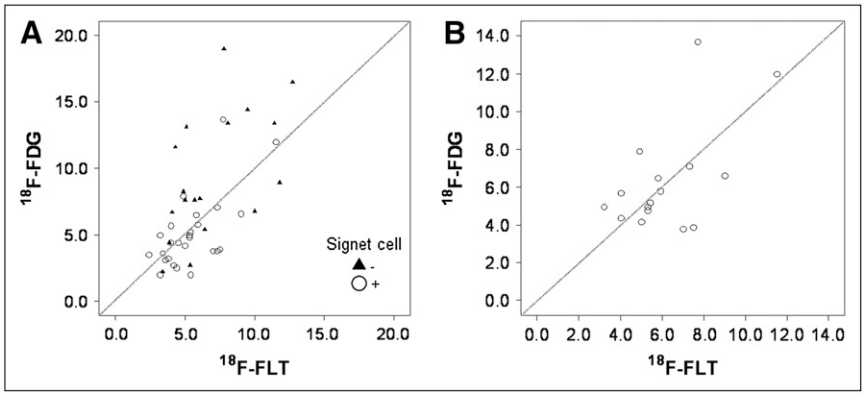


**FIGURE 2.** Correlation of SUV means for $^{18}$F-FLT and $^{18}$F-FDG in subgroup of $^{18}$F-FDG–positive patients ($n = 31$) (A) and subgroup of signet ring cell carcinomas positive for $^{18}$F-FDG PET uptake ($n = 16$) (B).

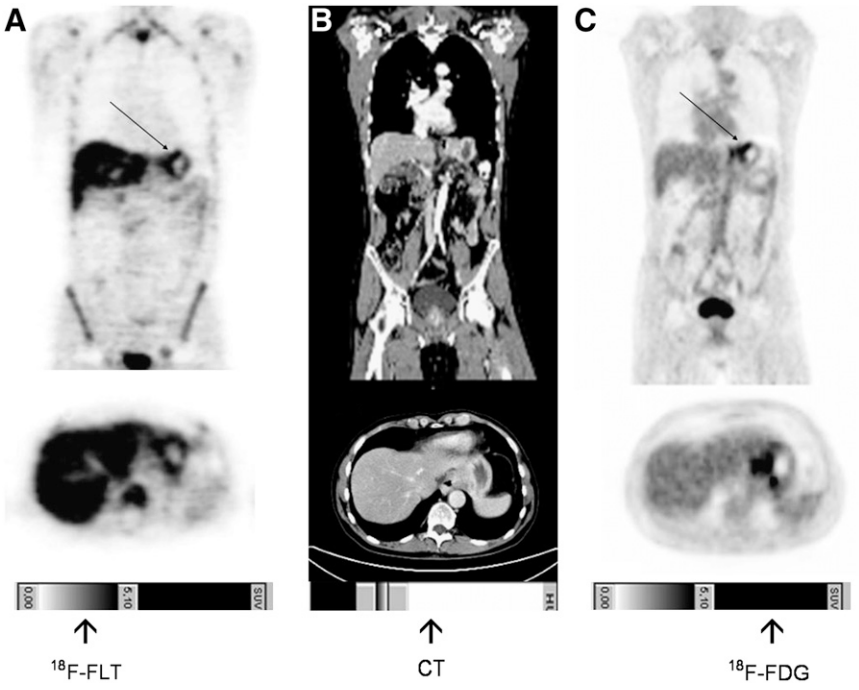


**FIGURE 3.** Coronal and transversal $^{18}$F-FLT PET (A), conventional CT (B), and $^{18}$F-FDG PET (C) views of patient with gastric cancer (linitis plastica, arrow).

significantly influencing uptake of $^{18}$F-FLT, as was also shown previously for $^{18}$F-FDG (*21*).

Several limitations have to be considered when our results are transferred to the clinic. Our results apply to a specific group of patients with a high proportion of signet ring cell–containing tumors, reflecting a patient selection different from that of previous studies (*21*). However, the fact that our results were found exactly for this group of patients indicates that $^{18}$F-FLT PET may be used for imaging gastric cancer containing signet ring cells—a histologic subtype with a markedly reduced sensitivity on $^{18}$F-FDG PET. Furthermore, the impact of $^{18}$F-FLT PET for imaging locally advanced gastric cancers is rather limited considering that detection and diagnosis of gastric cancer remains the domain of conventional imaging modalities such as endoscopy, endoscopic ultrasound, and CT. However, studies investigating the role of $^{18}$F-FLT PET for monitoring therapy of gastric cancers may strongly influence clinical management.

Our study documents that $^{18}$F-FLT PET is a feasible tool for imaging tumors of an unfavorable histologic type (signet ring cell carcinoma) and low $^{18}$F-FDG uptake. $^{18}$F-FDG has been used successfully for treatment monitoring of adenocarcinomas of the esophagogastric junction and gastric cancers (*14,20,21,27,28*). However, some tumors have uptake insufficient to provide the image contrast needed for quantitative analysis of $^{18}$F-FDG PET. This pilot study provides the rationale for future use of $^{18}$F-FLT for treatment monitoring because all primaries could be visualized with $^{18}$F-FLT, suggesting that $^{18}$F-FLT PET can be used to tailor treatment to the chemosensitivity of an individual tumor.

## CONCLUSION

In summary, this clinical study compared $^{18}$F-FLT PET with $^{18}$F-FDG PET for the detection of locally advanced gastric cancer. $^{18}$F-FLT PET had a higher sensitivity than $^{18}$F-FDG PET and might serve as a useful diagnostic adjunct for the quantitative assessment of proliferation. In the future, the addition of $^{18}$F-FLT PET to $^{18}$F-FDG PET could improve early evaluation of the response to neoadjuvant treatment of gastric cancer.

## ACKNOWLEDGMENTS

We appreciate the excellent contributions made by our colleagues Petra Watzlowik, Karin Kantke, and Michael Herz and the great support by Christine Praus and our technical staff members Brigitte Dzewas and Coletta Kruschke.

## REFERENCES

1. Chen J, Cheong JH, Yun MJ, et al. Improvement in preoperative staging of gastric adenocarcinoma with positron emission tomography. *Cancer.* 2005;103:2383–2390.
2. Kim SK, Kang KW, Lee JS, et al. Assessment of lymph node metastases using $^{18}$F-FDG PET in patients with advanced gastric cancer. *Eur J Nucl Med Mol Imaging.* 2006;33:148–155.
3. Mochiki E, Kuwano H, Katoh H, Asao T, Oriuchi N, Endo K. Evaluation of $^{18}$F-2-deoxy-2-fluoro-D-glucose positron emission tomography for gastric cancer. *World J Surg.* 2004;28:247–253.
4. Yoshioka T, Yamaguchi K, Kubota K, et al. Evaluation of $^{18}$F-FDG PET in patients with advanced, metastatic, or recurrent gastric cancer. *J Nucl Med.* 2003;44:690–699.
5. Yun M, Lim JS, Noh SH, et al. Lymph node staging of gastric cancer using $^{18}$F-FDG PET: a comparison study with CT. *J Nucl Med.* 2005;46:1582–1588.

6. De Potter T, Flamen P, Van Cutsem E, et al. Whole-body PET with FDG for the diagnosis of recurrent gastric cancer. *Eur J Nucl Med Mol Imaging.* 2002;29: 525–529.
7. Stahl A, Ott K, Weber WA, et al. FDG PET imaging of locally advanced gastric carcinomas: correlation with endoscopic and histopathological findings. *Eur J Nucl Med Mol Imaging.* 2003;30:288–295.
8. Buck AC, Schirrmeister HH, Guhlmann CA, et al. Ki-67 immunostaining in pancreatic cancer and chronic active pancreatitis: does in vivo FDG uptake correlate with proliferative activity? *J Nucl Med.* 2001;42:721–725.
9. Shields AF, Grierson JR, Dohmen BM, et al. Imaging proliferation in vivo with [F-18]FLT and positron emission tomography. *Nat Med.* 1998;4:1334–1336.
10. Lin PF, Zhao SY, Ruddle FH. Genomic cloning and preliminary characterization of the human thymidine kinase gene. *Proc Natl Acad Sci USA.* 1983;80:6528–6532.
11. Weber G, Nagai M, Natsumeda Y, et al. Regulation of de novo and salvage pathways in chemotherapy. *Adv Enzyme Regul.* 1991;31:45–67.
12. Wells P, Aboagye E, Gunn RN, et al. 2-[$^{11}$C]thymidine positron emission tomography as an indicator of thymidylate synthase inhibition in patients treated with AG337. *J Natl Cancer Inst.* 2003;95:675–682.
13. Francis DL, Freeman A, Visvikis D, et al. In vivo imaging of cellular proliferation in colorectal cancer using positron emission tomography. *Gut.* 2003;52:1602–1606.
14. van Westreenen HL, Cobben DC, Jager PL, et al. Comparison of $^{18}$F-FLT PET and $^{18}$F-FDG PET in esophageal cancer. *J Nucl Med.* 2005;46:400–404.
15. Wieder HA, Geinitz H, Rosenberg R, et al. PET imaging with [(18)F]3′-deoxy-3′-fluorothymidine for prediction of response to neoadjuvant treatment in patients with rectal cancer. *Eur J Nucl Med Mol Imaging.* 2007;34:878–883.
16. Jonasson L, Hallgrimsson J, Olafsdottir G. Gastric carcinoma: correlation of diagnosis based on biopsies and resection specimens with reference to the Lauren classification. *APMIS.* 1994;102:711–715.
17. Machulla HJ, Blocher A, Kuntzsch M, Piert M, Wei R, Grierson JR. Simplified labeling approach for synthesizing 3′-deoxy-3′-[$^{18}$F]fluorothymidine ([$^{18}$F]FLT). *J Radioanal Nucl Chem.* 2000;243:843–846.
18. Herrmann K, Wieder HA, Buck AK, et al. Early response assessment using 3′-deoxy-3′-[$^{18}$F]fluorothymidine-positron emission tomography in high-grade non-Hodgkin's lymphoma. *Clin Cancer Res.* 2007;13:3552–3558.
19. Weber WA, Ziegler SI, Thodtmann R, Hanauske AR, Schwaiger M. Reproducibility of metabolic measurements in malignant tumors using FDG PET. *J Nucl Med.* 1999;40:1771–1777.
20. Buck AK, Halter G, Schirrmeister H, et al. Imaging proliferation in lung tumors with PET: $^{18}$F-FLT versus $^{18}$F-FDG. *J Nucl Med.* 2003;44:1426–1431.
21. Ott K, Fink U, Becker K, et al. Prediction of response to preoperative chemotherapy in gastric carcinoma by metabolic imaging: results of a prospective trial. *J Clin Oncol.* 2003;21:4604–4610.
22. Flier JS, Mueckler MM, Usher P, Lodish HF. Elevated levels of glucose transport and transporter messenger RNA are induced by ras or src oncogenes. *Science.* 1987;235:1492–1495.
23. Kawamura T, Kusakabe T, Sugino T, et al. Expression of glucose transporter-1 in human gastric carcinoma: association with tumor aggressiveness, metastasis, and patient survival. *Cancer.* 2001;92:634–641.
24. Napieralski N, Ott K, Kremer M, et al. Methylation of tumor related genes in neoadjuvant treated gastric cancer: relation to therapy response, clinicopathological and molecular features. *Clin Cancer Res.* 2007. In press.
25. Ott K, Vogelsang H, Mueller J, et al. Chromosomal instability rather than p53 mutation is associated with response to neoadjuvant cisplatin-based chemotherapy in gastric carcinoma. *Clin Cancer Res.* 2003;9:2307–2315.
26. Perumal M, Pillai RG, Barthel H, et al. Redistribution of nucleoside transporters to the cell membrane provides a novel approach for imaging thymidylate synthase inhibition by positron emission tomography. *Cancer Res.* 2006;66:8558–8564.
27. Ott K, Weber WA, Lordick F, et al. Metabolic imaging predicts response, survival, and recurrence in adenocarcinomas of the esophagogastric junction. *J Clin Oncol.* 2006;24:4692–4698.
28. Weber WA, Ott K, Becker K, et al. Prediction of response to preoperative chemotherapy in adenocarcinomas of the esophagogastric junction by metabolic imaging. *J Clin Oncol.* 2001;19:3058–3065.

JNM The Journal of NUCLEAR MEDICINE

# Imaging Gastric Cancer with PET and the Radiotracers $^{18}$F-FLT and $^{18}$F-FDG: A Comparative Analysis

Ken Herrmann, Katja Ott, Andreas K. Buck, Florian Lordick, Dirk Wilhelm, Michael Souvatzoglou, Karen Becker, Tibor Schuster, Hans-Jürgen Wester, Jörg R. Siewert, Markus Schwaiger and Bernd J. Krause

*J Nucl Med.* 2007;48:1945-1950.
Published online: November 15, 2007.
Doi: 10.2967/jnumed.107.044867



*The Journal of Nuclear Medicine* is published monthly.
SNMMI | Society of Nuclear Medicine and Molecular Imaging
1850 Samuel Morse Drive, Reston, VA 20190.
(Print ISSN: 0161-5505, Online ISSN: 2159-662X)



SNMMI SOCIETY OF NUCLEAR MEDICINE AND MOLECULAR IMAGING